Quantum Noise Theory of Exceptional Point Amplifying Sensors

Mengzhen Zhang, William Sweeney, Chia Wei Hsu, Lan Yang, A. D. Stone, and Liang Jiang

Phys. Rev. Lett. **123**, 180501 — Published 29 October 2019

DOI: 10.1103/PhysRevLett.123.180501

Quantum Noise Theory of Exceptional Point Amplifying Sensors

Mengzhen Zhang,[1,2] William Sweeney,[1,2] Chia Wei Hsu,[1,2,3] Lan Yang,[4] A. D. Stone,[1,2] and Liang Jiang*[1,2,5]

[1] *Departments of Applied Physics and Physics, Yale University, New Haven, CT 06520, USA*
[2] *Yale Quantum Institute, Yale University, New Haven, CT 06520, USA*
[3] *Ming Hsieh Department of Electrical and Computer Engineering, University of Southern California, Los Angeles, California 90089, USA*
[4] *Department of Electrical and Systems Engineering, Washington University, St Louis, Missouri 63130, USA*
[5] *Pritzker School of Molecular Engineering, The University of Chicago, Chicago, Illinois 60637, USA*

Open quantum systems can have exceptional points (EPs), degeneracies where both eigenvalues and eigenvectors coalesce. Recently, it has been proposed and demonstrated that EPs can enhance the performance of sensors in terms of amplification of a detected signal. However, typically amplification of signals also increases the system noise, and it has not yet been shown that an EP sensor can have improved signal to noise performance. We develop a quantum noise theory to calculate the signal-to-noise performance of an EP sensor. We use the quantum Fisher information to extract a lower bound for the signal-to-noise ratio (SNR) and show that parametrically improved SNR is possible. Finally, we construct a specific experimental protocol for sensing using an EP amplifier near its lasing threshold and heterodyne signal detection that achieves the optimal scaling predicted by the Fisher bound. Our results can be generalized to higher order EPs for any bosonic non-Hermitian system with linear interactions.

A distinct feature of physical systems described by non-Hermitian operators are exceptional points (EPs), degeneracies at which not only eigenvalues but also the eigenstates coalesce [1–4] enhancing the repulsion and leading to a larger frequency splitting when detuned. EPs have been extensively discussed in the context of generalizing the standard quantum theory to include non-Hermitian Hamiltonians [5]. However even within the conventional quantum framework, the effect of EPs in *open* systems can already be studied, either by looking at resonant scattering or by treating unobserved degrees of freedom as lossy or amplifying reservoirs, as reviewed in [6]. Many interesting effects of EPs have been studied in electromagnetic or optomechanical systems [7–13]; often these systems have parity-time symmetry[8, 14–17], although this symmetry is not essential to the existence of EPs.

One intriguing application of EPs is to enhance the performance of sensors, which has been theoretically proposed [18–20] and experimentally demonstrated using optical micro-ring resonators [21, 22]. In these sensors the small parameter ϵ to be estimated acts as a perturbation to the system Hamiltonian, which is non-Hermitian due to intrinsic loss. For example, in optical-cavity systems, thermal effects or cavity shape deformation shift the complex resonant frequencies of the cavity, which can be measured by locating the centers and widths of the peaks in the frequency spectrum of the scattered output signal. If the unperturbed Hamiltonian is not at an EP initially, those frequencies will be shifted by amounts proportional to ϵ. Now we create an EP by tuning the initial Hamiltonian with additional non-Hermitian dynamics (e.g. extra lossy or gain channels), bringing two or more resonances to degeneracy without imposing any additional symmetries. The perturbation theory of EP's leads to a novel phenomenon: if n resonances have coalesced at an $n-1$th-order EP, then the eigen-frequency difference $\delta\omega$ of two of the perturbed resonances is proportional to $\epsilon^{1/n}$. Therefore, the sensitivity of the splitting to the perturbative strength $d(\delta\omega)/d\epsilon \propto \epsilon^{(1-n)/n}$, which tends to infinity when ϵ tends to 0, is parametrically larger than for non-EP systems, and hence proposed as a promising approach for enhancing sensing precision [18–20]. This type of enhanced frequency sensitivity was demonstrated in the micro-ring experiments [21, 22], where fabrication and fine-parameter-tuning of EP are already available in laboratories.

But there has been no systematic analysis of the effect on the noise and the signal-to-noise ratio (SNR) of a sensor operating in the vicinity of an EP. According to quantum noise theory [23], the gain (and loss) introduced by non-Hermitian dynamics will unavoidably generate additional noise. For example, in the context of the bounded modes of cavities with extrinsic pumping, the perturbation near EP amplifies both the mode amplitude and the added quantum noise to the same degree, making it dubious that the SNR will be enhanced [24] (assuming the sensor is operating near the quantum noise limit, and is not dominated by extrinsic noise sources). In quantum sensing, the close relation between SNR and the ultimate precision threshold has been pointed out [25]. Therefore, in evaluating the efficacy of EP sensors, it is crucial to understand the behavior of both signal and noise near an EP.

In this Letter, we address the following questions: (1) Can operating near an EP enhance the SNR of a sensor? (2) What is the maximal precision (in terms of SNR) of EP sensing schemes? (3) How can we design a scheme to achieve this ultimate precision? To answer them, we first apply quantum noise theory [23] to calculate the ampli-

tude and covariance matrix associated with the outputs of an EP sensor; then calculate the quantum Fisher information of the output state and obtain the Cramér–Rao bound for the parameter estimation. Finally we explicitly construct an amplifying EP sensor achieving this optimal sensitivity scaling, using muti-mode heterodyne detection (i.e. measuring a specific vector $\mu_{\rm out}$ of the scattered output signal, known in optics as *quadratures*), ideally at the lasing threshold. Our scheme does not use frequency splitting near an EP, but rather the amplitude change (i.e. $d\mu_{\rm out}/d\epsilon$) of an amplified superposition of output quadratures, which is our output signal, near the lasing frequency, with the system tuned to the lasing threshold, i.e. in the parameter regime where the imaginary part of the resonant eigen-frequency vanishes.

The conventional defintion of SNR is compatible only with scalar-form signals. Because of the vector-form output signal in our system, we modify the conventional definition to a multivariate form, namely $(d\mu_{\rm out}/d\epsilon)^T\mathbf{V}_{\rm out}^{-1}(d\mu_{\rm out}/d\epsilon)$ with $\mathbf{V}_{\rm out}$ the covariance matrix of the output signal $\mu_{\rm out}$. For convenience we will also call this modified measure the SNR [26]. Later, we will show its close relation to the quantum Fisher information, analogous to what is known in quantum sensing [25]. The results can be generalized to higher-order EPs for any bosonic non-Hermitian system with linear interactions, i.e. involving only Gaussian processes [27]. There are already studies on open system quantum metrology where decoherence is typically modelled in the form of Lindbladian master equations or completely-positive-and-trace-preserving (CPTP) maps, but these have not given a clear and explicit treatment for non-Hermitian systems [28–32]. The methods of quantum metrology are also routinely applied to the optimization of sensors [33–35], but these studies are not focused on noisy Gaussian quantum systems.

Non-Hermitian dynamics and open quantum systems. We define a non-Hermitian Hamiltonian to characterize the open system [6]. A generic model is shown in Fig. 1a; we have coupled cavities with two resonant modes a_1 and a_2, with the non-Hermitian hamiltonian (setting $\hbar = 1$)

$$\hat{H} = (\omega_1+\epsilon)\,\hat{a}_1^\dagger\hat{a}_1 + (\omega_2+\epsilon)\,\hat{a}_2^\dagger\hat{a}_2 + g\left(\hat{a}_1^\dagger\hat{a}_2 + h.c.\right) - i\frac{\gamma_1}{2}\hat{a}_1^\dagger\hat{a}_1 + i\frac{\gamma_2}{2}\hat{a}_2^\dagger\hat{a}_2, \tag{1}$$

where the total loss/gain rates of modes 1, 2 are γ_1, γ_2 and g is the inter-cavity coupling. Assume that the real parts of the resonance frequencies can be tuned to $\omega_1 = \omega_2 = \omega$, and the perturbation to be sensed uniformly shifts the frequencies of both modes by ϵ. The resulting equation of motion in the classical limit is

$$\frac{d}{dt}\begin{pmatrix} a_1 \\ a_2 \end{pmatrix} = -i\begin{pmatrix} (\omega+\epsilon) - i\frac{\gamma_1}{2} & g \\ g & (\omega+\epsilon) + i\frac{\gamma_2}{2} \end{pmatrix}\begin{pmatrix} a_1 \\ a_2. \end{pmatrix} \tag{2}$$

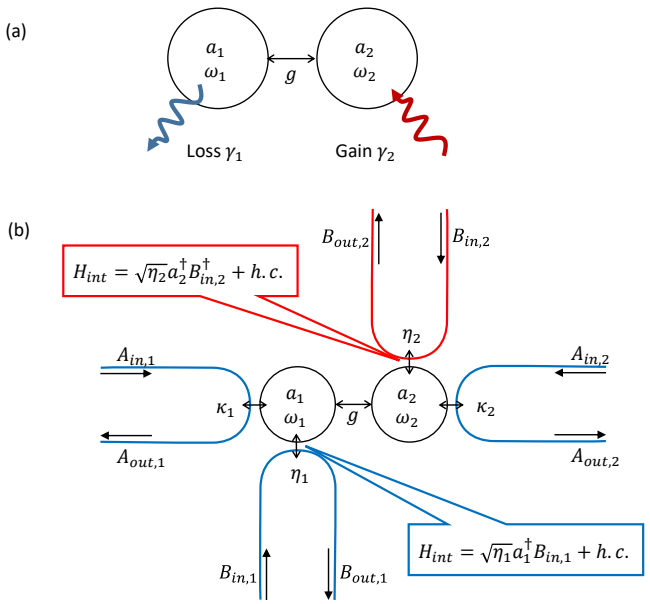

Figure 1. **(a).** Schematic of two-bosonic-mode system with loss and gain modeled classically. **(b).** Schematic of two-bosonic-mode system with a full quantum description. The circles labeled represent two bosonic modes a_1 and a_2, coupled to probing channels A_1 and A_2. In addition to the probing channels, a_1 is intrinsically dissipated by scattering channel B_1 and a_2 is intrinsically amplified by scattering channel B_2, with different coupling interactions. The arrows in the channels which point towards the system modes represent the input modes, while those with opposite direction represent the output modes.

The above equation is characterized by the 2×2 matrix derived from the non-Hermitian Hamiltonian. It has an EP [6] when the condition $(\gamma_2+\gamma_1)^2/16 = |g|^2$ is satisfied, where the originally orthogonal eigen-modes of this equation of motion coalesce to a single mode with resonant frequency $\Omega = (\omega+\epsilon+i(\gamma_2-\gamma_1))/4$. Note that if $\gamma_2 = \gamma_1$ is also satisfied, Ω is real and hence called the *lasing frequency*. EP-enhanced sensing will be achieved by monitoring the quadrature amplitudes associated with a_1, a_2 at fixed ω as the EP (and lasing frequency) is shifted by the perturbation ϵ. Due to the EP, the resonance amplitude falls off as ϵ^{-2}, leading to higher sensitivity. However Eq. 2 only describes the average behavior near the EP and not the noise properties.

The imaginary parts of the coupling rates γ_1, γ_2 arise from a combination of outcoupling to the probe channels A_1, A_2 with rates κ_1, κ_2, and loss and gain processes in the cavities with rates η_1, η_2 [36]. For simplicity we assume $\kappa_1 = \kappa_2 = \kappa$. Hence, the total loss and gain rates are $\gamma_1 = \eta_1 + \kappa$ and $\gamma_2 = \eta_2 - \kappa$ for the two modes, respectively. We denote $A_{1,\rm in(out)}$ and $A_{2,\rm in(out)}$ for the complex amplitudes of the two input (output) probe channels, satisfying the input-output relation $(A_{1,\rm out}, A_{2,\rm out}) = (A_{1,\rm in}, A_{2,\rm in}) + \sqrt{\kappa}(a_1, a_2)$. To

fully characterize the noise properties, we also need to model the fluctuations associated with the intrinsic loss η_1 and gain η_2. As shown in Fig. 1b, this can be done by introducing two auxiliary scattering channels B_1 and B_2 to simulate the intrinsic dissipation and amplification processes in a_1 and a_2. According to quantum noise theory [23], B_1 is coupled to a_1 via a beam-splitter-type interaction $\hat{B}_1^\dagger \hat{a}_1 + h.c.$ with coupling strength $\sqrt{\eta_1}$, while B_2 is coupled to a_2 via a squeezer-type interaction $\hat{B}_2^\dagger \hat{a}_2^\dagger + h.c.$ with coupling strength $\sqrt{\eta_2}$. The quantum Langevin equations for both modes are

$$\begin{aligned}
&\frac{d}{dt}\begin{pmatrix}\hat{a}_1\\ \hat{a}_2\end{pmatrix}\\
=&-i\begin{pmatrix}(\omega+\epsilon)-i\frac{\gamma_1(\kappa,\eta_1)}{2} & g\\ g & (\omega+\epsilon)+i\frac{\gamma_2(\kappa,\eta_2)}{2}\end{pmatrix}\begin{pmatrix}\hat{a}_1\\ \hat{a}_2\end{pmatrix}\\
&+\begin{pmatrix}\sqrt{\kappa}\hat{A}_{1,\mathrm{in}}\\ \sqrt{\kappa}\hat{A}_{2,\mathrm{in}}\end{pmatrix}+\begin{pmatrix}\sqrt{\eta_1}\hat{B}_{1,\mathrm{in}}\\ -\sqrt{\eta_2}\hat{B}_{2,\mathrm{in}}^\dagger\end{pmatrix},
\end{aligned}\tag{3}$$

which now has additional noise $\hat{B}_{1,\mathrm{in}}$, $\hat{B}_{2,\mathrm{in}}^\dagger$ compared with Eq. (2), inducing dependence of γ_1, γ_2 on κ, η_1 and η_2.

Amplitude vector and covariance matrix. To model the dissipation and amplification, we can simply set the channels B_1 and B_2 to zero average amplitudes, i.e. vacuum. For any pair of bosonic annihilation and creation operators $\hat{a}$ and $\hat{a}^\dagger$, we define a pair of "position" and "momentum" quadrature operators $\hat{q} = \hat{a} + \hat{a}^\dagger$ and $\hat{p} = -i\left(\hat{a} - \hat{a}^\dagger\right)$ [27]. Given any state of N modes, the amplitude vector μ and covariance matrix $\mathbf{V}$ can be defined in the quadrature basis $\mu_j = \langle \hat{\mathbf{x}}_j \rangle$ and $\mathbf{V}_{j,k} = \frac{1}{2}\langle \hat{\mathbf{x}}_j \hat{\mathbf{x}}_k + \hat{\mathbf{x}}_k \hat{\mathbf{x}}_j \rangle - \langle \hat{\mathbf{x}}_j \rangle \langle \hat{\mathbf{x}}_k \rangle$, for $1 \le j,k \le N$, with vector $\hat{\mathbf{x}} = (\hat{q}_1, \hat{q}_2, \ldots, \hat{q}_N, \hat{p}_1, \hat{p}_2, \ldots, \hat{p}_N)^T$, and $\langle\cdot\rangle$ the expectation value [27].

To compute them, we perform the Fourier transform of Eq. (3) to obtain the relation between the Fourier transformed operators $\hat{A}[\omega] \equiv \int \hat{A}(t) e^{-i\omega t} dt$ of the input and output ports. The amplitude vector and covariance matrix of the probe output channels are [37]

$$\mu_{\mathrm{out}} = (\mathbf{I} - \mathbf{G}_\theta)\,\mu_{\mathrm{in}}, \tag{4}$$

$$\mathbf{V}_{\mathrm{out}} = (\mathbf{I} - \mathbf{G}_\theta)\,\mathbf{V}_{\mathrm{in}}\,(\mathbf{I} - \mathbf{G}_\theta)^T + \mathbf{G}_\theta \mathbf{R} \mathbf{V}'_{\mathrm{in}} \mathbf{R}^T \mathbf{G}_\theta^T, \tag{5}$$

where

$$\theta = \epsilon/\kappa \tag{6}$$

is the *dimensionless perturbation strength*, μ_{in} and $\mathbf{V}_{\mathrm{in}}$ are the amplitude vector and covariance matrix of the probe input channels ($A_{1,\mathrm{in}}[\omega]$, $A_{2,\mathrm{in}}[\omega]$), $\mathbf{V}'_{\mathrm{in}}$ is the covariance matrix of the auxiliary input channels ($B_1[\omega]$, $B_2[-\omega]$), $\mathbf{R} = \mathrm{diag}\left\{\sqrt{\eta_1}, -\sqrt{\eta_2}, \sqrt{\eta_1}, \sqrt{\eta_2}\right\}$. The *dimensionless linear response matrix* $\mathbf{G}_\theta$ [37] is

$$\mathbf{G}_\theta = -\mathbf{\Omega}\,(\theta\mathbf{I} - \mathbf{M})^{-1}, \tag{7}$$

where the *symplectic form* $\mathbf{\Omega} = (0, \mathbf{I}; -\mathbf{I}, 0)$, and the 4×4 matrix $\mathbf{M} = (0, G, \Gamma_1, 0; G, 0, 0 - \Gamma_2; G, 0, 0, -\Gamma_2; -\Gamma_1, 0, 0, G; 0, \Gamma_2, G, 0)$ is the *dimensionless* effective Hamiltonian in quadrature basis [39] with dimensionless parameters $\Gamma_1 = \gamma_1/(2\kappa)$, $\Gamma_2 = \gamma_2/(2\kappa)$, and $G = g/\kappa$.

For most applications, it is sufficient to consider Gaussian states for the probe and auxiliary input channels. Since $\hat{H}$ involves only linear interactions between modes, the output states are also Gaussian, and are completely characterized by the μ_{out} and $\mathbf{V}_{\mathrm{out}}$ [27]. Hence, the above calculations are sufficient to characterize the performance of sensing.

EP sensing. By choosing $\Gamma_1 = \Gamma_2 = G$ the system will be at the lasing threshold and will remain at an EP as the perturbation shifts the lasing frequency shifted by θ (the situation where the system is not exactly at the lasing threshold will be discussed later). We then have a non-trivial Jordan decomposition of the matrix $\mathbf{M} = \mathbf{P}\mathbf{\Lambda}\mathbf{P}$ with an invertible matrix $\mathbf{P}$ [40], and $\mathbf{\Lambda} = (0,1,0,0;0,0,0,0;0,0,0,1;0,0,0,0)$.

For small perturbation $\theta \ll 1$, the response matrix grows as a polynomial of θ^{-1}

$$\begin{aligned}
\mathbf{G}_\theta &= -\mathbf{\Omega}\,(\theta\mathbf{I} - \mathbf{M})^{-1} = -\theta^{-1}\sum_{n=0}^{\infty}\theta^{-n}\mathbf{\Omega}\mathbf{M}^n\\
&= -\theta^{-1}\mathbf{\Omega} - \theta^{-2}\mathbf{\Omega}\mathbf{M},
\end{aligned}\tag{8}$$

where the second equality uses the Taylor expansion and the third equality uses $\mathbf{M}^n = 0$ for $n \ge 2$. The first and second terms of $\mathbf{G}_\theta$ are due to lasing threshold and EP respectively. The second term implies an enhanced output signal (the amplitude vector [Eq. (4)]) at ω as $\theta \to 0$. However, the noise (the covariance matrix [Eq. (5)]) contains a θ^{-4} term because of its dependence on $\mathbf{G}_\theta$ [37], and hence diverges as $\theta \to 0$. Therefore one might expect that there is no hope of enhancing the sensitivity of the signal with respect to the noise. However, systematic calculation of the uncertainty of the measured parameter θ in the presence of noise shows this is not necessarily true. In the following, we first provide a lower bound to sensitivity using the quantum Cramér–Rao bound and then provide an EP sensing protocol which achieves the same θ-scaling as that bound.

Sensitivity lower bound. In the presence of noise, the standard deviation of the estimates of the parameter θ, calculated from data obtained from some measurement, is bounded by the inverse of the quantum Fisher information $\mathcal{I}(\theta)$ of the state through the quantum Cramér–Rao inequality [41]

$$\delta\theta \ge \mathcal{I}(\theta)^{-1/2}. \tag{9}$$

For Gaussian processes (e.g. our scheme), the quantum Fisher information [42, 43] takes the form $\mathcal{I}(\theta) = \mathcal{I}_{\mathbf{V}}(\theta) + \mathcal{I}_{\mu}(\theta)$, where $\mathcal{I}_{\mathbf{V}}(\theta)$ is always positive and only

depends on $\mathbf{V}_{\text{out}}$, and

$$\mathcal{I}_{\mu}(\theta)=\left(\frac{d\mu_{\text{out}}}{d\theta}\right)^{T}\mathbf{V}_{\text{out}}^{-1}\frac{d\mu_{\text{out}}}{d\theta}. \tag{10}$$

Since $\mathcal{I}_{\mathbf{V}}(\theta)$ is only determined by fluctuations in the absence of the probe, the quantum Fisher information is dominated by $\mathcal{I}_{\mu}(\theta)$ for sufficiently strong input probes. Eq. (10) is the SNR generalized to be compatible with vector-form inputs, as alluded to in the introduction.

We plug Eqs. (4, 5&8) into Eq. (10) and obtain [37]

$$\mathcal{I}_{\mu}(\theta)=\theta^{-4}\left(c_0+O[\theta]\right), \tag{11}$$

implying the leading contribution to the quantum Fisher information scales at least as θ^{-4} (orange curve (——) in Fig. 2) and the sensitivity, $\delta\theta\geq c_0\times\theta^2$, with constant $c_0>0$ determined by the choice of input probe signals in generic situations [37]. This EP-enhanced behavior is compared with a non-EP scheme (with $g=\eta_1=0$) which shows no enhancement as $\theta\to 0$ (the solid green curve (——) in Fig. 2). Hence, EP sensing has a more favorable lower bound than the conventional protocols.

One can intuitively understand the improvement by EP as a result of correlations between different eigenmodes of the output state. Due to the EP structure of the matrix $\mathbf{G}_{\theta}$, different linear combinations of the quadratures will accumulate noise with different θ-dependence. For our system, only two orthogonal directions in the four-dimensional input space lead to noise amplified by θ^{-4} [37]; thus there is a large remaining subspace of inputs for which the SNR is enhanced by operating at or near an EP.

Heterodyne detection to achieve optimized EP sensing scaling. The Cramér–Rao bound applies to all possible sensing schemes; now we provide a specific EP sensing scheme that achieves the same scaling predicted by the Cramér–Rao bound. The idea is to use heterodyne measurement to extract the output amplitude vector μ_{out}. The covariance matrix associated with the heterodyne detection is $\mathbf{V}_{\text{out}}+\mathbf{I}$ [37, 44], which includes the additional quantum noise inherent in the simultaneous measurement of both position and momentum quadratures. Fortunately, this additional noise has no θ-dependence, and becomes negligibly small compared to $\mathbf{V}_{\text{out}}$ for $\theta\to 0$. Hence, we have $\left(\mathbf{V}_{\text{out}}+\mathbf{I}\right)^{-1}=\mathbf{V}_{\text{out}}^{-1}\left(\mathbf{I}+O[\theta]\right)\approx\mathbf{V}_{\text{out}}^{-1}$.

For example, by injecting a coherent state with $\mu_{\text{in}}=\mathbf{P}\cdot(0,1,0,0)^{T}$, the heterodyne detection can measure the output amplitude vector $\mu_{\text{out}}=(\mathbf{I}-\mathbf{G}_{\theta})\mu_{\text{in}}=\mu_{\text{in}}-\mathbf{\Omega P}\cdot\left(\theta^{-2},\theta^{-1},0,0\right)^{T}$. We can obtain uncertainty $\delta\theta\approx\mathcal{I}_{\mu}(\theta)^{-1/2}\sim\theta^2$, which has the same scaling as the lower bound obtained from Eqs. (9,10,11).

General approach and higher-order EP sensing. We summarize our general approach to achieve EP sensing with the same scaling as the Cramér–Rao bound. For an EP sensing scheme based on a Gaussian process, we calculate the corresponding matrices to track the change of amplitude and covariance matrix. Then we can calculate the quantum Fisher information and obtain the precision bound. Generally, $\mathbf{G}_{\theta}=-\mathbf{\Omega}\left(\theta\mathbf{\Pi}-\mathbf{M}\right)^{-1}$ (in our previous discussion, $\mathbf{\Pi}=\mathbf{I}$, but it is invertible in general), and $\mathbf{M\Pi}^{-1}=\mathbf{P}\Lambda\mathbf{P}^{-1}$, with $\mathbf{P}$ invertible , and $\mathbf{\Lambda}$ known as the Jordan normal form of $\mathbf{M\Pi}^{-1}$ consisting of diagonal blocks of size N_i (for the ith block), each with eigenvalue zero. When $N_i=1$, the corresponding block is just a scalar, which is not an EP. To have EP enhanced sensing, we need at least one non-trivial Jordan block ($N_i\geq 2$) with eigenvalue zero.

Let $N=\max_i N_i$ be the size of the largest zero-eigenvalue Jordan block, corresponding to the $(N-1)$-th order EP. Then it is easy to show that $\mathbf{G}_{\theta}=\theta^{-N}\left(-\mathbf{\Omega C}_0+O(\theta)\right)+\cdots$ with $\theta\to 0$ with $\mathbf{C}_0$ a constant matrix. This divergence near $\theta=0$ leads to θ^{-N} amplification of the amplitude and θ^{-2N} amplification of the covariance matrix. One might be tempted to argue that the $\mathcal{I}_{\mu}(\theta)$ is then proportional to θ^{-2} since the scaling of amplification with N can be perfectly canceled by covariance matrix. However, a more rigorous calculation shows this is overly pessimistic. As $d\mathbf{G}_{\theta}/d\theta=\mathbf{G}_{\theta}\mathbf{\Pi\Omega G}_{\theta}$, only one $\mathbf{G}_{\theta}$ cancels with the amplification in the covariance matrix. We have $\mathcal{I}_{\mu}(\theta)=\mu_{\text{in}}^{T}\mathbf{G}_{\theta}^{T}\mathbf{C}_1\mathbf{G}_{\theta}\mu_{\text{in}}$, where $\mathbf{C}_1$ is a positive-definite matrix [37]. So $\mathcal{I}_{\mu}(\theta)\approx\theta^{-2N}$ for $(N-1)$-th order EP. Since $\mathcal{I}_{\mathbf{V}}(\theta)$ is always positive, $\mathcal{I}_{\mu}(\theta)$ gives a lower bound on quantum Fisher informa-

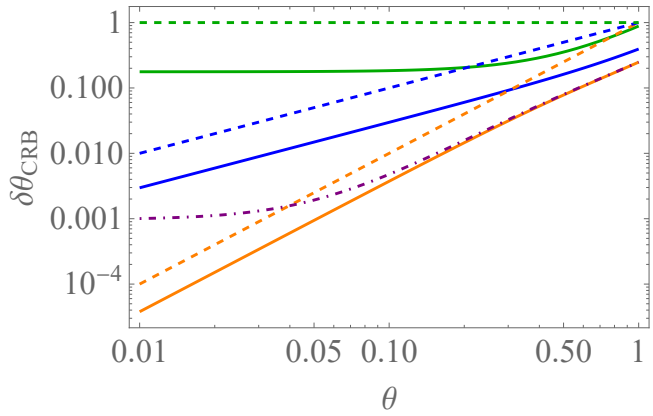

Figure 2. Smallest achievable standard variations determined by the Cramér–Rao-bound). All solid curves: minimal standard variation of parameter θ. Solid orange (——): two-mode EP sensing at the lasing threshold with all modes perturbed. Solid blue (——): two-mode EP sensing at lasing threshold with only one mode perturbed. Solid green (——): single-mode conventional sensing, no additional loss or gain. Dashed orange (– – –), blue (– – –), and green (– – –): reference lines for θ^2, θ^1, and θ^0 scaling. Dot-dashed purple (– · –): two-mode EP sensing below lasing threshold, with additional loss $\delta=0.05\Gamma$ added to each cavity.

tion. We have then the quantum Cramér–Rao bound $\delta\theta \gtrsim \theta^N$ [45], the scaling of which can be achieved by performing heterodyne measurement on all of the outputs even in this general situation.

Robustness of enhanced sensing The key conditions for enhanced sensing are precise tuning to an EP and operating the sensor at the lasing threshold. As noted above, when satisfied, there are a large family of input states generating enhanced sensitivity for appropriately chose outputs, i.e. the sensor is robust to the choice of input state. While operation at the lasing threshold condition is assumed in order to derive the results above, we can actually relax this condition, and still achieve sensitivity enhancement over some parameter range. A small perturbation δ from the lasing threshold will simply suppress the enhanced sensing θ below some cutoff. As shown in purple curve (— · — · —) in Fig. 2, when we introduce additional loss δ to both cavities, the quantum Fisher information is upper bounded by $\mathcal{I}^{UB} \approx \|\mathbf{G}_{\theta=0}\|^2 \approx \delta^{-4}$, where $\|\cdot\|$ represents the trace norm [37]. So long as the system is sufficiently close to the lasing threshold ($\delta \ll \theta$), the quantum Fisher information does not exceed the upper bound ($\mathcal{I} \approx \theta^{-4} \ll \mathcal{I}^{UB}$), and the EP supports enhanced SNR. Generally, for higher order EPs, we will have EP-enhanced sensing near the lasing threshold as long as the additional loss δ is much smaller than the signal θ [37].

In conclusion, we have established a theoretical framework using quantum noise theory to calculate systematically both the signal and noise of EP sensors operating near the lasing threshold. Using the quantum Fisher information, we have obtained the lower bound of ultimate sensitivity of EP-sensors. Moreover, we provide a heterodyne detection scheme to achieve the optimal scaling of the sensitivity predicted by this bound. Since these EP sensors are described by Gaussian processes with linear interactions, EP sensing near the laser threshold coupled with heterodyne detection should be feasible with current experimental techniques, such as the micro resonators of [21, 22].

Note added: During the completion of this work, we became aware of several related but different studies [46, 47]. In Lau and Clerk's work [46], the authors are proposing another way of achieving enhanced precision limit, i.e., by constructing non-reciprocal coupling with the reservoir, while the function of EPs and lasing threshold are not discussed. In [47] by Chen, et.al., although a two-mode EP sensor is studied, the authors did not mention the function of lasing threshold.

We would like to thank Aash Clerk, Hoi-Kwan Lau, Jack Harris, Jianming Wen, and Peter Rabl for discussions. We also acknowledge support from the ARL-CDQI, ARO (W911NF-14-1-0011, W911NF-16-1-0563), AFOSR MURI (FA9550-14-1-0052, FA9550-15-1-0015), ARO MURI (W911NF-16-1-0349), NSF (EFMA-1640959, DMR-1743235), Alfred P. Sloan Foundation (BR2013-0049), and Packard Foundation (2013-39273).

[1] T. Kato, *Perturbation theory for linear operators*, vol. 132 (Springer Science & Business Media, 2013).
[2] W. D. Heiss, Eur. Phys. J. D-Atomic, Mol. Opt. Plasma Phys. **7**, 1 (1999).
[3] W. Heiss, Physical Review E **61**, 929 (2000).
[4] M. V. Berry, Czechoslovak journal of physics **54**, 1039 (2004).
[5] N. Moiseyev, *Non-Hermitian quantum mechanics* (Cambridge University Press, 2011).
[6] R. El-Ganainy, K. G. Makris, M. Khajavikhan, Z. H. Musslimani, S. Rotter, and D. N. Christodoulides, Nature Physics **14**, 11 (2018).
[7] Z. Lin, H. Ramezani, T. Eichelkraut, T. Kottos, H. Cao, and D. N. Christodoulides, Phys. Rev. Lett. **106**, 213901 (2011).
[8] L. Chang, X. Jiang, S. Hua, C. Yang, J. Wen, L. Jiang, G. Li, G. Wang, and M. Xiao, Nature photonics **8**, 524 (2014).
[9] B. Peng, k. K. Özdemir, F. Lei, F. Monifi, M. Gianfreda, G. L. Long, S. Fan, F. Nori, C. M. Bender, and L. Yang, Nature Physics **10**, 394 (2014).
[10] H. Xu, D. Mason, L. Jiang, and J. Harris, Nature **537**, 80 (2016).
[11] J. Doppler, A. A. Mailybaev, J. Böhm, U. Kuhl, A. Girschik, F. Libisch, T. J. Milburn, P. Rabl, N. Moiseyev, and S. Rotter, Nature **537**, 76 (2016).
[12] K. G. Makris, R. El-Ganainy, D. Christodoulides, and Z. H. Musslimani, Physical Review Letters **100**, 103904 (2008).
[13] B. Zhen, C. W. Hsu, Y. Igarashi, L. Lu, I. Kaminer, A. Pick, S.-L. Chua, J. D. Joannopoulos, and M. Soljačić, Nature **525**, 354 (2015).
[14] C. E. Rüter, K. G. Makris, R. El-Ganainy, D. N. Christodoulides, M. Segev, and D. Kip, Nature physics **6**, 192 (2010).
[15] A. Regensburger, C. Bersch, M.-A. Miri, G. Onishchukov, D. N. Christodoulides, and U. Peschel, Nature **488**, 167 (2012).
[16] L. Feng, Z. J. Wong, R.-M. Ma, Y. Wang, and X. Zhang, Science **346**, 972 (2014).
[17] Z. Zhang, Y. Zhang, J. Sheng, L. Yang, M.-A. Miri, D. N. Christodoulides, B. He, Y. Zhang, and M. Xiao, Physical review letters **117**, 123601 (2016).
[18] J. Wiersig, Physical Review Letters **112**, 203901 (2014).
[19] J. Wiersig, Physical Review A **93**, 033809 (2016).
[20] Z.-P. Liu, J. Zhang, k. K. Özdemir, B. Peng, H. Jing, X.-Y. Lü, C.-W. Li, L. Yang, F. Nori, and Y.-x. Liu, Physical review letters **117**, 110802 (2016).
[21] W. Chen, k. K. Özdemir, G. Zhao, J. Wiersig, and L. Yang, Nature **548**, 192 (2017).
[22] H. Hodaei, A. U. Hassan, S. Wittek, H. Garcia-Gracia, R. El-Ganainy, D. N. Christodoulides, and M. Khajavikhan, Nature **548**, 187 (2017).
[23] C. Gardiner and P. Zoller, *Quantum noise: a handbook of Markovian and non-Markovian quantum stochastic methods with applications to quantum optics*, vol. 56 (Springer Science & Business Media, 2004).
[24] W. Langbein, Phys. Rev. A **98**, 023805 (2018),

URL https://link.aps.org/doi/10.1103/PhysRevA.98.023805.

[25] C. L. Degen, F. Reinhard, and P. Cappellaro, Rev. Mod. Phys. **89**, 035002 (2017), URL https://link.aps.org/doi/10.1103/RevModPhys.89.035002.

[26] The name is justified by comparing it to the traditional SNR with signal replaced by the differential signal $d\mu_{\rm out}/d\epsilon$. This form also resembles the Mahalanobis distance in statistics as a measure of likelihood for multivariate normal distributions, which is widely used in cluster analysis and classification.

[27] C. Weedbrook, S. Pirandola, R. García-Patrön, N. J. Cerf, T. C. Ralph, J. H. Shapiro, and S. Lloyd, Rev. Mod. Phys. **84**, 621 (2012).

[28] A. W. Chin, S. F. Huelga, and M. B. Plenio, Phys. Rev. Lett. **109**, 233601 (2012), URL https://link.aps.org/doi/10.1103/PhysRevLett.109.233601.

[29] M. Tsang, New Journal of Physics **15**, 073005 (2013), URL https://doi.org/10.1088%2F1367-2630%2F15%2F7%2F073005.

[30] S. Alipour, M. Mehboudi, and A. T. Rezakhani, Phys. Rev. Lett. **112**, 120405 (2014), URL https://link.aps.org/doi/10.1103/PhysRevLett.112.120405.

[31] S. Gammelmark and K. Mølmer, Phys. Rev. Lett. **112**, 170401 (2014), URL https://link.aps.org/doi/10.1103/PhysRevLett.112.170401.

[32] S. A. Haine and S. S. Szigeti, Phys. Rev. A **92**, 032317 (2015), URL https://link.aps.org/doi/10.1103/PhysRevA.92.032317.

[33] S. M. Assad, M. Bradshaw, and P. K. Lam, International Journal of Quantum Information **15**, 1750009 (2017).

[34] C. A. Weidner and D. Z. Anderson, Phys. Rev. Lett. **120**, 263201 (2018), URL https://link.aps.org/doi/10.1103/PhysRevLett.120.263201.

[35] M. Kritsotakis, S. S. Szigeti, J. A. Dunningham, and S. A. Haine, Phys. Rev. A **98**, 023629 (2018), URL https://link.aps.org/doi/10.1103/PhysRevA.98.023629.

[36] We note that when $\kappa_1 = \kappa_2$ the EP of the scattering matrix (e.g. $\mathbf{I} - \mathbf{G}_\theta$ in Eq. 4) is exactly the same as the EP of the non-Hermitian Hamiltonian . However, when $\kappa_1 \neq \kappa_2$, the EP of the scattering matrix is different from the EP of the non-Hermitian Hamiltonian. More details of the scattering matrix can be found in [37]. The distinction of different EPs is not the focus of this paper, and it will be discussed in another work.

[37] See Supplemental Material for further details, which includes [38].

[38] S.-i. Amari, *Information Geometry and Its Applications*, vol. 194 of *Applied Mathematical Sciences* (Springer Japan, Tokyo, 2016), ISBN 978-4-431-55977-1 978-4-431-55978-8.

[39] It is the matrix obtained from the Fourier transform of Eq. 2 represented in the quadrature basis, normalized by the coupling rate. More details can be found in [37].

[40] For real matrix $\mathbf{M}$, there exists a real invertible matrix $\mathbf{P}$ such that $\mathbf{P^{-1}MP}$ is a real block diagonal matrix with each block a real Jordan block. Such a real Jordan form is sufficient for our investigation of EP sensing.

[41] S. L. Braunstein and C. M. Caves, Phys. Rev. Lett. **72**, 3439 (1994).

[42] Z. Jiang, Phys. Rev. A **89**, 032128 (2014).

[43] A. Monras, arXiv:1303.3682 (2013).

[44] U. Leonhardt and H. Paul, Progress in Quantum Electronics **19**, 89 (1995).

[45] Actually, we can show that the "$\approx$" sign holds if the process is very noisy [37].

[46] H.-K. Lau and A. A. Clerk, Nature communications **9**, 4320 (2018).

[47] C. Chen, L. Jin, and R.-B. Liu, arXiv preprint arXiv:1809.05719 (2018).